

STRUCTURAL STUDIES OF STRESS ANNEALED $\text{Co}_{21}\text{Fe}_{64-x}\text{Nb}_x\text{B}_{15}$ ALLOYS

S. N. Kane¹, S. S. Khinchi², Zs. Gercsi³, A. Gupta⁴, L. K. Varga⁵
and F. Mazaleyrat^{6,7}

¹School of Physics, D. A. University, Khandwa road Campus, Indore-452001, India

²Department of Physics, Inst. of Eng. Tech., D. A. University, Indore-452001, India

³National Institute for Materials Science, Sengen 1-2-1, Tsukuba 305-0047, Japan

⁴UGC-DAE Consortium for Scientific Res., Univ. Campus, Khandwa road, Indore-452001, India

⁵RISSPO, Hungarian Academy of Sciences, P.O. Box 49, 1525 Budapest, Hungary

⁶Ecole Normale Supérieure de Cachan, SATIE UMR CNRS 8029, 94235 Cachan, France

⁷IUFM de Créteil, 94861 Bonneuil-sur-Marne Cedex, France

Received: March 29, 2008

Abstract. Influence of Nb content on structural properties of stress annealed $\text{Co}_{21}\text{Fe}_{64-x}\text{Nb}_x\text{B}_{15}$ ($x = 3, 5, 7$) alloys has been studied using differential scanning calorimetry, in-situ length change measurements during annealing, X-ray diffraction and Mössbauer spectroscopy. Results show that, increase of Nb content in the alloy increases the stability of the alloy against crystallization and is also responsible for higher elongation of the specimens. Crystallization leads to the formation of bcc Fe-Co nano-granular phase containing Co up to 30% and affects the spin texture.

Stress annealing of magnetic materials is known to induce significant uniaxial magnetic anisotropy. In materials consisting of α -Fe type nanoparticles dispersed in an amorphous matrix, this treatment can result in a strong anisotropy. In FINEMET type alloys (FeSiBNbCu), the stress-induced anisotropy is perpendicular ($K_V < 0$) to tensile stress direction [1] and strong ($\sim 10 \text{ J.m}^{-3} \text{ MPa}^{-1}$) whereas Co substitution turns it to longitudinal direction ($K_V > 0$) for 20 to 50% Co substituted to Fe [2]. The sign of uniaxial anisotropy coefficient is generally the same as that of the magnetostriction coefficient of the nanograins. However, for some alloys (FeZrB NANOPERM or 80% Co substituted FINEMET) the direction of the anisotropy is opposite to expectations [2]. It seems that this phenomenon is linked to the viscous behavior of the amorphous phase in the supercooled liquid region, i.e., between the glass transition and crystallization temperatures (T_g

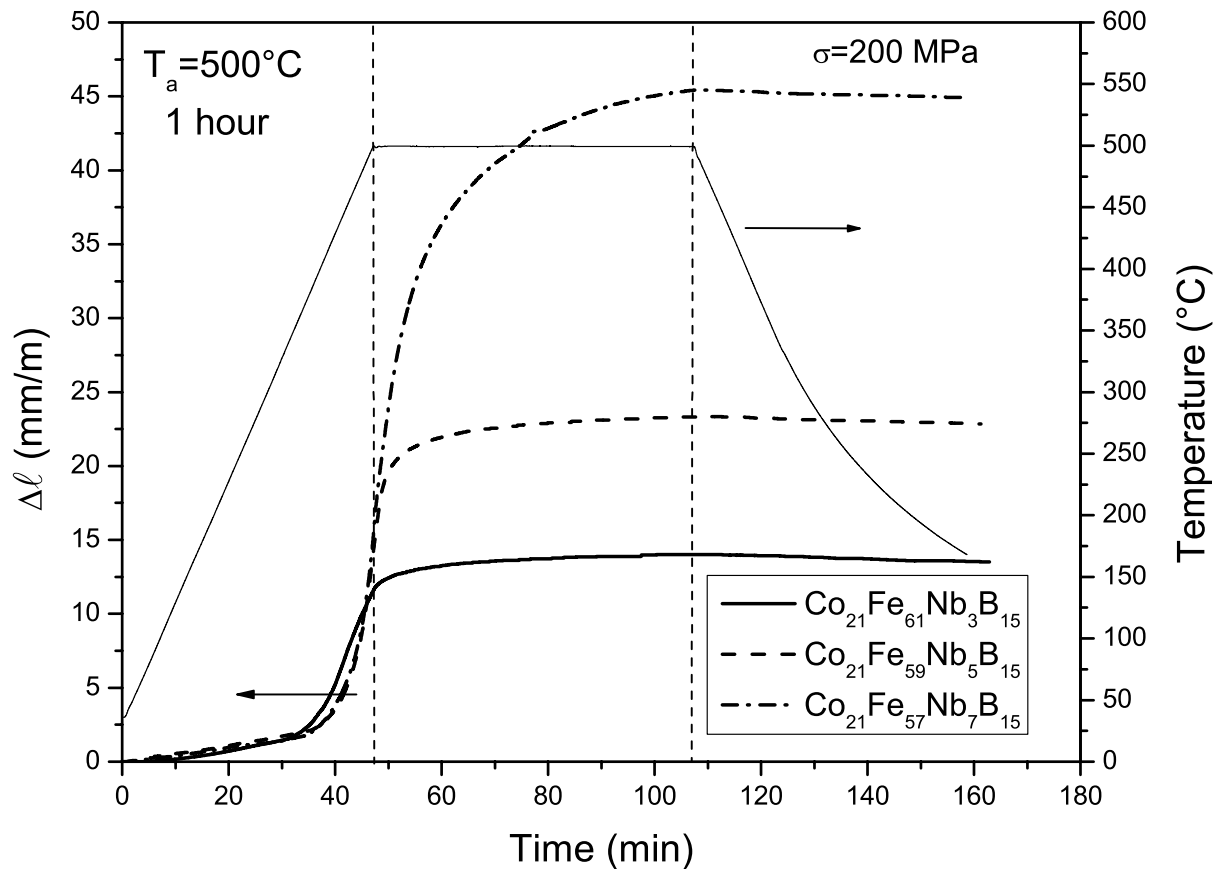
and T_x respectively). To have insight to this problem, it is necessary to study alloys with different $T_x - T_g$ values. In the present work we study the influence of Nb content on structural properties of stress annealed $\text{Co}_{21}\text{Fe}_{64-x}\text{Nb}_x\text{B}_{15}$ ($x = 3, 5, 7$) alloys using differential scanning calorimetry (DSC), in-situ length change measurements during annealing, X-ray diffraction (XRD) and Mössbauer spectroscopy.

Ribbons of nominal composition $\text{Co}_{21}\text{Fe}_{64-x}\text{Nb}_x\text{B}_{15}$ with $x = 3, 5, 7$ (about 20 μm thick and 10 mm wide) were prepared using a planar flow casting technique on copper wheel. First crystallization peak temperature (T_{x1}) was determined using DSC measurements performed at a heating rate of 20 $^\circ\text{C}/\text{min}$. Specimens were annealed at 450, 500, and 550 $^\circ\text{C}$ with applied stress of 200 MPa for 1 h in the protective atmosphere of flowing Ar. The elongation (Δl) of 1 m long ribbons was

Corresponding author: F. Mazaleyrat, e-mail: Frederic.MAZALEYRAT@satie.ens-cachan.fr

Table 1. Thermodynamical (T_x , T_g) and structural (a , D , and V_x) parameters for stress annealed $\text{Co}_{21}\text{Fe}_{64-x}\text{Nb}_x\text{B}_{15}$ specimens.

Nb (at.%)	T_g (°C)	T_x (°C)	$T_x - T_g$ (°C)	Ann. Temp (°C)	Δl (mm)	a (nm) ± 0.0001	D (nm) ± 2	V_x (%) ± 2
3	342	408	66	450	10.4	0.2869	30	45
				500	14.1	0.2867	35	55
				550	17.9	0.2867	38	55
5	384	442	58	450	12.9	0.2870	15	15
				500	13.4	0.2869	16	45
				550	27.2	0.2864	15	60
7	397	475	78	450	10.7	-	-	-
				500	45.4	0.2862	10	25
				550	>50	0.2862	15	55

**Fig. 1.** Elongation (ΔL) for $\text{Co}_{21}\text{Fe}_{64-x}\text{Nb}_x\text{B}_{15}$ alloys after annealing at 500 °C.

measured during annealing by means of a Linear Variable Differential Transformer. Recording Δl and temperature was performed using a PC linked

GPIB standard card as a function of time at a rate of 1 point/s during the whole thermal treatment (heating at 10 K/min, plateau at T_A , cooling at 10 K/

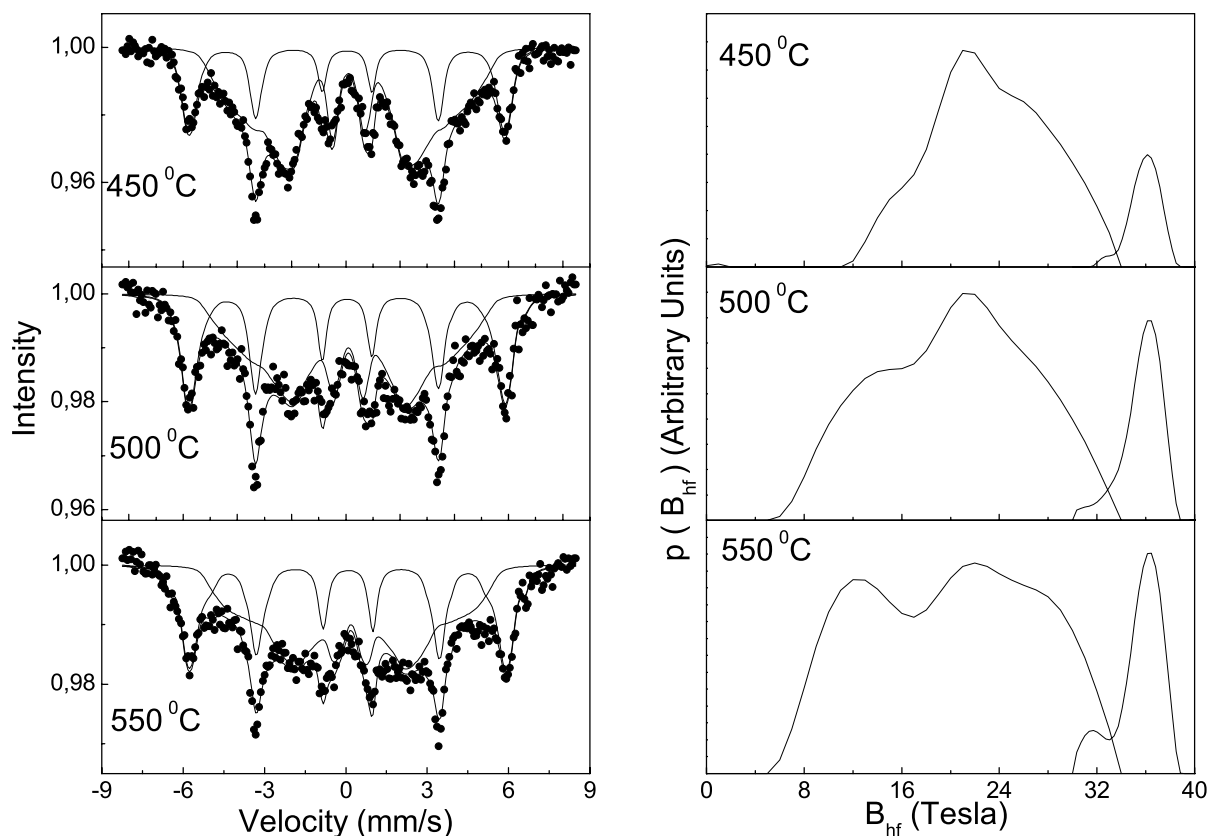


Fig. 2. Mössbauer spectra and corresponding hyperfine field distributions for stress annealed $\text{Co}_{21}\text{Fe}_{61}\text{Nb}_x\text{B}_{15}$ alloys.

min). CuK_α XRD measurements were done at room temperature, and were analyzed using pseudo-Voigt line profile to obtain lattice parameter a and average grain size (D) and the volume fraction of the nanograins (V_x). Transmission Mössbauer spectra were recorded at room temperature, using $^{57}\text{Co}:\text{Rh}$ source. Mössbauer spectra consisting of overlapped amorphous and crystalline components were fitted with distribution of hyperfine fields using NORMOS program.

T_{x1} for samples with $x = 3, 5,$ and 7 are respectively $408, 442$ and 475 °C, showing that increase of Nb content increases the stability of the alloy against crystallization. Fig. 1 shows the elongation (Δl) for $\text{Co}_{21}\text{Fe}_{64-x}\text{Nb}_x\text{B}_{15}$ during the annealing cycle (mentioned above). Perusal of Fig. 1 shows that, higher the Nb content in the alloy higher is the elongation of the alloy. T_g is deduced from the plot of dl/dt , which is the viscous flow speed. Below T_g , this speed is small and equal for all samples (0.5 mm/min). After correction of the thermal dilatation

($\sim 5 \cdot 10^{-6} \text{K}^{-1}$), the constant viscosity ($\sim 0.5 \cdot 10^{-12} \text{Pa}\cdot\text{s}$) is attributed to short range ordering [3].

Maximum flow speed was 60 mm/min for $x=7\%$ and the viscosity fell down to $4 \cdot 10^{-9} \text{Pa}\cdot\text{s}$ at 500 °C. The higher elongation is observed for the same sample due to the increase of crystallization temperature, enhancing the supercooled liquid region. It is important to note that application of stress modifies the total free energy of the metastable amorphous phase resulting in a lower T_g compared to measurements performed by DSC.

XRD data shows that the crystallization of the specimens starts after annealing at 450 °C with 200 MPa stress (except for the specimen with $x=7$, where crystallization starts after annealing of the specimen after 500 °C) showing a co-existence of the crystalline phase and the residual amorphous matrix. Table 1 depicts the Scherrer's crystallite size (D), lattice parameter (a) and volume fraction of the nano-grains (V_x) obtained by fitting the XRD data. In the early stage of crystallisation (450°C),

lattice parameters are rather high which suggests the precipitation of bcc Fe nano-granular phase with rather low Co content (15%) and a substantial lattice expansion that can be due to the presence of Nb solute atoms. As the annealing temperature increases, lattice parameters become consistent with bulk values and indicate a Co content of 15-20%, 30%, and 35% for $x=3, 5,$ and $7,$ respectively. As Nb content in the specimen increases, for same annealing temperature ' D ' is systematically smaller for the sample containing higher Nb content. V_x shows similar behavior for the studied samples. Behavior of D and V_x can be understood in terms of increase of T_{x1} values with increase of Nb content in the alloy.

Mössbauer measurements confirm that the crystallization of the specimens starts after annealing at $450\text{ }^\circ\text{C}$ with 200 MPa stress (except for the specimen with $x = 7$), showing a coexistence of the crystalline phase and the residual amorphous matrix. Fig. 2 shows the representative Mössbauer spectra (experimental data and fit) and specimens corresponding hyperfine field distributions for $\text{Co}_{21}\text{Fe}_{61}\text{Nb}_3\text{B}_{15}$ annealed with 200 MPa stress at various temperatures. Fig. 2 shows that increase of annealing temperature gives rise to higher crystalline component in the specimen. In hyperfine field distribution, a low field hump around 12 Tesla is observed and becomes more pronounced when the annealing temperature increases which is consistent with its attribution to iron atoms having Nb atoms in their first near-neighbor shell [4]. Relative intensity of the 2nd and 5th line, b is a measure of the spin texture of the sample relative to the direction of the γ -rays. For all samples, ' b ' indicates a random distribution in the nanograin. In contrast, spins in the amorphous phase are mainly in-plane for $T_A=450\text{ }^\circ\text{C}$ ($4 < b < 3$) and goes gradually to random for higher temperatures ($b \sim 2$). Notable excep-

tion is found for 7% Nb alloy for which ' b '=0.78 for $T_A=550\text{ }^\circ\text{C}$ indicating that spins are partly off-plane in the amorphous phase. Hyperfine field (B_{hf}) values for residual amorphous matrix ranges between 15.74 to 24.16 (± 0.2 Tesla), which are consistent with the presence of B as Fe near neighbors. B_{hf} values for the crystalline component between 35.53 and 37.03 (± 0.2 Tesla) suggest that the Co content ranges between 12 to 30% [5].

In conclusion, higher Nb content in the alloy increases the stability of the alloy against crystallization and is also responsible for the obtained higher elongation of the alloy through the enhancement of the supercooled liquid region. Crystallization of the studied alloys affects their spin texture in the amorphous matrix showing that the higher the elongation, the more spin texture is out of ribbon plane.

ACKNOWLEDGEMENT

SNK acknowledges gratefully one-month hospitality as invited professor at ENS de Cachan, Cachan (France).

REFERENCES

- [1] A.A. Glaser, N.M. Kleynerman, V.A. Lukshina, A.P. Patapov and V.V. Serikov // *Phys. Met. Metal.* **72** (1991) 53.
- [2] Zs. Gercsi, S. N. Kane, J. M. Greneche, L. K. Varga and F. Mazaleyrat // *Phys. Stat. Sol. (C)* **1** (2004) 3607.
- [3] G. Vlasák, P. Svec and P. Duha // *Mat. Sci. Eng. A* **304-306** (2001) 472.
- [4] A. Gupta, S. N. Kane, N. Bhagat and T. Kulik // *J. Magn. Magn. Mater.* **254-255** (2003) 492.
- [5] C. E. Johnson, M. S. Ridout, T.E. Cranshaw and P. E. Madsen // *Phys. Rev. Lett.* **6** (1961) 450.